European Journal of Pharmaceutics and Biopharmaceutics 199 (2024) 114293

Contents lists available at ScienceDirect

European Journal of Pharmaceutics and Biopharmaceutics

journal homepage: www.elsevier.com/locate/ejpb

Research paper

# Bioequivalence risk assessment of oral formulations containing racemic ibuprofen through a chiral physiologically based pharmacokinetic model of ibuprofen enantiomers

Javier Reig-López [a,b,1], Marina Cuquerella-Gilabert [a,b,c,1], Enrique Bandín-Vilar [d,e,f], Matilde Merino-Sanjuán [a,b], Víctor Mangas-Sanjuán [a,b,*], Alfredo García-Arieta [g]

[a] Department of Pharmacy and Pharmaceutical Technology and Parasitology, University of Valencia, Valencia, Spain
[b] Interuniversity Research Institute for Molecular Recognition and Technological Development, University of Valencia-Polytechnic University of Valencia, Spain
[c] Simulation Department, Empresarios Agrupados Internacional S.A., Madrid, Spain
[d] Pharmacy Department, University Clinical Hospital Santiago de Compostela (CHUS), Spain
[e] Clinical Pharmacology Group, Health Research Institute of Santiago de Compostela (IDIS), Spain
[f] Pharmacology, Pharmacy and Pharmaceutical Technology Department, Faculty of Pharmacy, University of Santiago de Compostela (USC), Spain
[g] Área de Farmacocinética y Medicamentos Genéricos, División de Farmacología y Evaluación Clínica, Departamento de Medicamentos de Uso Humano, Agencia Española de Medicamentos y Productos Sanitarios, Spain

ARTICLE INFO

*Keywords:*
Ibuprofen
PBPK
Bioequivalence
Stereoselectivity
Racemase

ABSTRACT

The characterization of the time course of ibuprofen enantiomers can be useful in the selection of the most sensitive analyte in bioequivalence studies. Physiologically based pharmacokinetic (PBPK) modelling and simulation represents the most efficient methodology to virtually assess bioequivalence outcomes. In this work, we aim to develop and verify a PBPK model for ibuprofen enantiomers administered as a racemic mixture with different immediate release dosage forms to anticipate bioequivalence outcomes based on different particle size distributions. A PBPK model incorporating stereoselectivity and non-linearity in plasma protein binding and metabolism as well as R-to-S unidirectional inversion has been developed in Simcyp®. A dataset composed of 11 Phase I clinical trials with 54 scenarios (27 per enantiomer) and 14,452 observations (7129 for R-ibuprofen and 7323 for S-ibuprofen) was used. Prediction errors for $AUC_{0-t}$ and $C_{max}$ for both enantiomers fell within the 0.8–1.25 range in 50/54 (93 %) and 42/54 (78 %) of scenarios, respectively. Outstanding model performance, with 10/10 (100 %) of $C_{max}$ and 9/10 (90 %) of $AUC_{0-t}$ within the 0.9–1.1 range, was demonstrated for oral suspensions, which strongly supported its use for bioequivalence risk assessment. The deterministic bioequivalence risk assessment has revealed R-ibuprofen as the most sensitive analyte to detect differences in particle size distribution for oral suspensions containing 400 mg of racemic ibuprofen, suggesting that achiral bioanalytical methods would increase type II error and declare non-bioequivalence for formulations that are bioequivalent for the eutomer.

*Abbreviations:* ADAM, advanced dissolution, absorption and metabolism model; ADME, absorption, distribution, metabolism and excretion; AFE, average fold error; AAFE, absolute average fold error; ARS, absorption rate scalar; $AUC_{0-t}$, area under the concentration–time profile from zero to last observation; $AUC_{Tmax}$, area under the concentration–time profile from zero to median time to peak plasma concentration of the reference formulation; BE, bioequivalence; $CL_{int}$, intrinsic clearance; $C_{max}$, peak plasma concentration; DLM, diffusion layer model; M&S, modelling and simulation; PBPK, physiologically-based pharmacokinetics; PK, pharmacokinetics; PE, prediction error; PPB, particle population balance; PPE, percent prediction error; PSD, particle size distribution; $T_{max}$, time to peak plasma concentration.

* Corresponding author at: Department of Pharmacy and Pharmaceutical Technology and Parasitology, University of Valencia, Av Vicent Andrés Estellés, s/n. 46100, Burjassot, Valencia, Spain.
*E-mail address:* victor.mangas@uv.es (V. Mangas-Sanjuán).
[1] Both authors contributed equally to this work.

https://doi.org/10.1016/j.ejpb.2024.114293
Received 20 February 2024; Received in revised form 26 March 2024; Accepted 15 April 2024
Available online 17 April 2024

## 1. Introduction

The granularity in the characterization of pharmacokinetic (PK) processes with the aim of understanding and predicting with a greater degree of certainty *what-if* scenarios in both drug development and clinical practice represents an inherent consequence of the consolidation of model-informed drug discovery and development (MID3) [1–4]. Physiologically-based pharmacokinetic (PBPK) modelling and simulation (M&S) represents a significant strategy within the MID3 umbrella, because of its efficiency in the management and integration of drug-, system-, and trial-related parameters into a model structure built up with anatomically differentiated compartments, physiologically representing organs and tissues [5–10]. This approach leads to complex and reliable mathematical frameworks with recognition by the main regulatory agencies [11–13]. One of the applications that has been emerging in recent years is focused on using PBPK models to predict the impact on bioavailability because of formulation changes in an already authorized medicine. However, this type of in silico strategies must demonstrate a high predictive performance, as regulatory decisions will be based on the assessment of its behavior in non-tested scenarios. For this reason, the development of highly predictive PBPK models based on extensive experimental evidence contributes to clarifying the role that this strategy can play in the field of bioequivalence (BE).

Ibuprofen is a chiral nonsteroidal anti-inflammatory drug (NSAID), which is typically administered as a racemic mixture of R- and S-ibuprofen free acid or arginine, lysine and sodium salts, but other options like guaiacol and pyridoxine esters, as well as isobutanol-ammonium and meglumine derivatives, are also available commercially [14]. According to the Biopharmaceutics Classification System, ibuprofen is a class IIa drug due to its low solubility in acidic media and high intestinal permeability [14,15]. Several model-informed strategies have been published in recent years to assess the impact of ibuprofen dissolution and/or absorption on the pharmacokinetic performance of different oral formulations [16,17]. PBPK models coupled with pharmacodynamic models have been developed for ibuprofen to confirm that the different rate of absorption translates into a different onset of action, which is clinically relevant for analgesic drugs [18]. In addition, an *in vitro-in vivo* extrapolation of dissolution integrated into a PBPK approach, considering a product-specific particle size distribution (PSD) and the self-buffering effect of the drug, has also been developed to support drug product development and manufacturing changes, setting clinically relevant specifications for immediate release (IR) formulations containing ibuprofen [19]. Dissolution methods have been developed to increase the discriminatory power of *in vitro* dissolution tests [16,20], since compendial media have shown the inability to detect differences in the peak and time to peak exposure between formulations of ibuprofen [21]. These dissolution methodologies were used to confirm and establish a level A *in vitro-in vivo* correlation with two ibuprofen IR products that had failed to show bioequivalence [22].

Ibuprofen is a chiral drug for which the two enantiomers have different pharmacodynamic activity since S-ibuprofen (eutomer) has been reported to be about 160 times more potent than R-ibuprofen (distomer) in inhibiting prostaglandin synthesis *in vitro* [23–25]. The potency of racemic ibuprofen is 0.5-fold the potency of S-ibuprofen in inhibiting platelet aggregation and thromboxane formation, while R-ibuprofen was about 100-fold less active [26]. Furthermore, R-ibuprofen is unidirectionally inverted to S-ibuprofen *in vivo* [27–29], and the rate of absorption and the route of administration seem to affect the extent of chiral inversion [30,31]. Despite the different model-informed strategies already published, no PBPK model has considered the chirality of ibuprofen or the kinetics of R-to-S inversion. Furthermore, the experimental data used in the above modelling strategies leads to a narrow design space, addressing only specific issues within the complex PK properties of ibuprofen oral formulations, thus negatively impacting their predictive performance. In this sense, a rational and sequential PBPK model development with sufficient experimental evidence would generate a workflow that facilitates credible risk assessment exercises.

Therefore, the objective of the present work was to develop a PBPK model for ibuprofen enantiomers administered as a racemic mixture intravenously (IV) and orally with different IR dosage forms (i.e., solutions, suspensions, tablets and soft gelatine capsules) in healthy volunteers (HV) in order to characterize the impact of chirality on the ADME processes and to anticipate BE outcomes based on the rate of absorption as a consequence of different PSD of ibuprofen enantiomers.

## 2. Materials and methods

### 2.1. Experimental dataset

A total of 278 individuals enrolled in 11 independent Phase I clinical trials providing 7,129 and 7,323 plasma observations for R- and S-ibuprofen, respectively, were used to develop and verify the PBPK models of ibuprofen enantiomers. This clinical dataset covered a wide range of scenarios with different routes of administration, dose levels, and formulations. HVs received racemic ibuprofen administration IV and orally in fasted state conditions. Study design characteristics as well as number of observations for each enantiomer are summarised in Table 1.

### 2.2. Modelling strategy

The analysis was conducted in Simcyp® Simulator [32,33] v21R1 following the workflow suggested by Kuepfer et al. [8], which increases model complexity step-by-step through an independent and sequential characterization and inclusion of PK processes. Briefly, unidirectional inversion of R-ibuprofen to S-ibuprofen was characterized after the IV administration of 100 mg of the pure enantiomer (i.e., R-ibuprofen). Disposition processes of ibuprofen enantiomers were finally verified using experimental IV data after the infusion of 400 and/or 600 mg of ibuprofen racemate. Then, the systemic exposure after the oral administration of solutions of ibuprofen racemate was assessed characterizing its absorption properties and the pre-systemic inversion of R-ibuprofen with the Advanced Dissolution, Absorption and Metabolism (ADAM) model [34]. Finally, different models of immediate release oral formulations were developed to best describe the exposure of ibuprofen enantiomers after the oral administration of suspension, soft gelatine capsules and tablets. A schematic representation of the modelling strategy is depicted in supplementary material Fig. 1 and fully described as follows. Final PBPK model parameters are shown in Table 2.

#### 2.2.1. IV formulation

Molecular weight (MW), lipophilicity (logP) and acidity ($pK_a$) of ibuprofen were incorporated as physicochemical properties and assumed to be the same for both enantiomers. A different concentration-dependent fraction unbound ($f_u$) in plasma was introduced into Simcyp® for each enantiomer to allow for a stereoselective and non-linear plasma protein binding process, as reported by Paliwal et al. [35]. The Rodgers and Rowland method to predict the volume of distribution at steady state ($V_{ss}$) was used [36,37]. A cytosolic racemase was considered to cover the complex process of R-ibuprofen chiral inversion to S-ibuprofen [38]. Setting S-ibuprofen as a primary metabolite of R-ibuprofen and considering chiral inversion contributes to 60 % of R-ibuprofen elimination [39], a value of 1.2 L/h (40 % of the systemic clearance estimated by Cheng et al. [40] was fixed as additional clearance for R-ibuprofen elimination. With this framework, a parameter estimation (PE) using the PE module within Simcyp® v21R1 of the intrinsic clearance ($CL_{int}$) through this racemase as well as the systemic clearance of the formed S-ibuprofen was performed using literature data after the administration of 100 mg of R-ibuprofen to HVs [40] (supplementary material Table 1). To further characterize ibuprofen enantiomers elimination, renal clearance ($CL_R$) and enzymatic parameters ($V_{max}$ and $K_M$) for cytochrome P450 (CYP) 2C8 and 2C9 as well as for

**Table 1**
Study characteristics and number of observations for R-ibuprofen and S-ibuprofen.

| Study | RoA | N | Femaleproportion (%) | Dose (mg) | Formulation | R-Ibu Obs | S-Ibu Obs | Additional information |
|---|---|---|---|---|---|---|---|---|
| A | IV<br>OR | 24 | 50 | 600,600 | Solution for infusion<br>Solution | 381<br>376 | 390<br>384 | Infusion times: 15, 20 and 30 min; oral solution of ibuprofen arginate |
| B | IV<br>OR | 24 | 50 | 600<br>600 | Solution for infusion<br>Solution | 390<br>400 | 394<br>404 | Infusion time: 30 min; oral solution of ibuprofen arginate |
| C | IV<br>OR | 24 | 33.33 | 400<br>400 | Solution for infusion<br>Solution | 376<br>374 | 384<br>384 | Infusion time: 30 min; oral solution of ibuprofen arginate |
| D | IV<br>OR | 35 | 48.57 | 400<br>400 | Solution for infusion<br>Solution | 672<br>692 | 698<br>720 | Infusion time: 30 min; oral solution of ibuprofen arginate |
| E | OR | 14 | 0 | 200 | Suspension | 481 | 516 | 2 % oral suspension |
| F | OR | 23 | 0 | 400 | Suspension | 1062 | 1079 | 2 % and 4 % oral suspensions |
| G | OR | 30 | 52 | 400 | Soft gelatine capsule | 31 | 30 | Lysine salt; mean profiles |
| H | OR | 26 | 54 | 400 | Soft gelatine capsule | 984 | 1000 | |
| I | OR | 24 | 50 | 600 | Tablet | 33 | 36 | Mean profiles |
| J | OR | 24 | 33 | 600 | Tablet | 877 | 904 | |
| K | OR | 30 | 0 | 600 | Tablet | – | – | Only PK exposure parameters available |

RoA: route of administration; N: number of individuals; R-Ibu Obs: number of R-ibuprofen observations; S-Ibu Obs: number of S-ibuprofen observations.

UDP-glucuronosyltransferases (UGT) 1A3, 1A9, 2B4 and 2B7 were incorporated into the model to account for the previously fixed R-ibuprofen additional clearance and the estimated S-ibuprofen systemic clearance. An additional human liver microsomes (HLM)-mediated $CL_{int}$ was finally incorporated to best describe the elimination of both enantiomers. Due to the lack of dose proportionality [38], data from studies A and C were used to confirm initial model parameterisation and refinement. In this regard, a tissue-to-plasma partition coefficient (Kp) scalar of 1.5 was used to capture the observed peak exposure ($C_{max}$) after the administration of the highest dose (i.e., 600 mg). Notwithstanding, the resulting $V_{ss}$ fell within the reported range of 0.1–0.2 L/kg [38], thus supporting the optimisation of this model parameter. Studies B and D were used to verify the predictive power of the PBPK models developed.

#### 2.2.2. Oral solution

Using the already characterized ibuprofen disposition processes, presystemic assessment of R-ibuprofen chiral inversion was performed with data from literature after the administration of 200 mg of R-ibuprofen as an oral solution [40]. Human jejunum effective permeability ($P_{eff,man}$) was predicted from apparent permeability ($P_{app}$) in Caco-2 cells and the ADAM model was selected to describe intestinal transit and absorption in each segment of the gastrointestinal tract. Mean gastric emptying time was optimised to a final value of 0.12 h to capture the observed time to peak exposure ($T_{max}$). Racemase intestinal activity scalar was set to 0 to best describe the observed data and predict R-ibuprofen oral bioavailability. Studies A and C were used to confirm model parameterisation and refinement. The ADAM model required an absorption rate scalar (ARS) of 10 in duodenum and jejunum to capture the high absorption rate observed in these studies in terms of $C_{max}$ and $T_{max}$, which could be explained by the presence of arginine in the formulation [38]. Studies B and D were also simulated to check model parameterisation and ARS and gastric emptying time optimisation and ultimately the predictive power of the mechanistic absorption model developed.

#### 2.2.3. Oral suspension

Increasing the complexity of the oral formulations, the dissolution process was added to the absorption model through a diffusion layer model (DLM) to better assess the characteristics of the oral suspension. Ibuprofen solubility as a function of pH was described through its intrinsic solubility ($S_0$) and a solubility factor of 79 as previously reported [19]. The particle population balance (PPB) model was selected as the DLM particle handing model, with a polydisperse PSD with a mean radius of 20 ± 5 μm [41], and the particle surface pH was modelled mechanistically to allow changes in surface concentration and dissolution rate as a direct consequence of ibuprofen dissolution (self-buffering effect). Pre-dissolved ibuprofen in the oral suspension was assumed to be negligible and thus a 0 % dissolved fraction was considered (local sensitivity analysis is provided in Table 2 and Fig. 2-5 of supplementary material). In the case of ibuprofen acid, the ARS in the segment jejunum I was set to 2 to best describe the absorption rate of both enantiomers. Study E (200 mg of racemic ibuprofen administered as a 2 % oral suspension) and study F (400 mg of racemic ibuprofen administered as a 2 % and 4 % oral suspension) were used to develop and verify the characteristics of the formulation, respectively.

#### 2.2.4. Soft gelatine capsule

Due to the rapid absorption of soft capsule formulations ($T_{max}$ of 0.6–0.7 h), the DLM model with the PSD previously developed for the oral suspension was considered. In the case of the formulation containing the lysine salt, the ARS in duodenum and jejunum previously optimized for the oral solution with arginine were used, and the pH-dependent solubility was directly described by its experimental solubility profile [16]. Soft capsules with ibuprofen acid were modelled with the same parameterization as the oral suspensions. Studies G and H were used to verify these assumptions.

#### 2.2.5. Tablets

IR tablets were developed adjusting the PSD to the values previously reported by Cristofoletti et al. [19]. Model development was performed with data from Study I, and Studies J and K were used to verify the predictive power of the systemic exposure to R- and S-ibuprofen by the PBPK models developed.

### 2.3. Simulations

All simulations consisted of 25 trials and equal study design (number of individuals and sampling times) and demographic characteristics of the corresponding population enrolled in the clinical study. Supplementary material Table 3 details all the information used for simulating each study in order to allow reproducibility of the work here presented.

**Table 2**
Final ibuprofen enantiomers PBPK model parameters.

| Parameter (Units) | R-ibuprofen | | S-ibuprofen | |
|---|---|---|---|---|
| | **Value** | **Source** | **Value** | **Source** |
| *Physicochemical Properties and Blood Binding* | | | | |
| MW (g/mol) | 206.29 | Drug bank | 206.29 | Drug bank |
| logP | 3.23 | [18] | 3.23 | [18] |
| Compound type | Monoprotic acid | | Monoprotic acid | |
| pKa | 4.5 | [18] | 4.5 | [18] |
| $S_0$ (mg/mL) | 0.043 | [19] | 0.043 | [19] |
| B/P | 0.55 | Assumed | 0.55 | Assumed |
| $f_{u,plasma}$ | Concentration dependent profile | [35] | Concentration dependent profile | [35] |
| *Absorption* | | | | |
| Model | ADAM | | ADAM | |
| $P_{app}$ 6.5:7.4 (Caco-2) ($10^{-6}$ cm/s) | 52.5 | [42] | 52.5 | [42] |
| $P_{eff,man}$ ($10^{-4}$ cm/s) | 6.81 | Simcyp predicted | 6.81 | Simcyp predicted |
| $k_a$ ($h^{-1}$) | 2.975 | Simcyp predicted | 2.975 | Simcyp predicted |
| Fu,GUT | 0.61117 | Simcyp predicted | 0.61117 | Simcyp predicted |
| ARS Duodenum | 1 (10 for arginine and lysine) | Optimized | 1 (10 for arginine and lysine) | Optimized |
| ARS Jejunum I | 2 (10 for arginine and lysine; 4 for soft capsules) | Optimized | 2 (10 for arginine and lysine; 4 for soft capsules) | Optimized |
| ARS Jejunum II | 1 (10 for arginine and lysine) | Optimized | 1 (10 for arginine and lysine) | Optimized |
| ARS Ileum I | 1 | Default | 1 | Default |
| ARS Ileum II | 1 | Default | 1 | Default |
| ARS Ileum III | 1 | Default | 1 | Default |
| ARS Ileum IV | 1 | Default | 1 | Default |
| ARS Colon | 1 | Default | 1 | Default |
| *Distribution* | | | | |
| Model | Minimal PBPK | | Minimal PBPK | |
| $V_{ss}$ (L/kg) | 0.0912490.11519 (600 mg) | Simcyp predicted | 0.091897 0.11616 (600 mg) | Simcyp predicted |
| Prediction Method | Rodgers and Rowland | [36,37] | Rodgers and Rowland | [36,37] |
| $K_p$ scalar | 1 (1.5 for 600 mg dose level) | Optimized | 1 (1.5 for 600 mg dose level) | Optimized |
| Elimination | | | | |
| Racemase $CL_{int}$ (μL/min/mg protein) | 87.25 | Estimated | – | – |
| CYP2C8 (2OH) $V_{max}$ (pmol/min/pmol) | 9.4 | [43] | 5.4 | [43] |
| CYP2C8 (2OH) $K_M$ (μM) | 282 | [43] | 292 | [43] |
| CYP2C9 (2OH) $V_{max}$ (pmol/min/pmol) | 17 | [43] | 16 | [43] |
| CYP2C9 (2OH) $K_M$ (μM) | 45 | [43] | 29 | [43] |
| CYP2C9 (3OH) $V_{max}$ (pmol/min/pmol) | 29 | [43] | 29 | [43] |
| CYP2C9 (3OH) $K_M$ (μM) | 45 | [43] | 40 | [43] |
| UGT1A3 $CL_{int}$ (μL/min/mg protein) | 0.4 | [44] | 0.4 | [44] |
| UGT1A9 $CL_{int}$ (μL/min/mg protein) | 2.2 | [44] | 2.2 | [44] |
| UGT2B4 $CL_{int}$ (μL/min/mg protein) | 0.3 | [44] | 0.3 | [44] |
| UGT2B7 $CL_{int}$ (μL/min/mg protein) | 8.9 | [44] | 8.9 | [44] |
| HLM additional $CL_{int}$ (μL/min/mg protein) | 70 | Optimised | 70 | Optimised |
| $CL_R$ (L/h) | 0.05 | [38] | 0.05 | [38] |
| *Formulation-related parameters* | | | | |
| | *Oral suspension* | *Soft gelatine capsule* | *Tablet* | |
| *Aqueous Phase Solubility* | | | | |
| Salt limited solubility factor | 79 [19] | 79 [19]<br>pH-dependent solubility for lysine salt [16] | 79 [19] | |
| Particle surface solubility | Surface pH<br>(Mechanistic model) | Surface pH<br>(Mechanistic model) | Surface pH<br>(Mechanistic model) | |

(*continued on next page*)

**Table 2** (*continued*)

| Parameter (Units) | R-ibuprofen | | S-ibuprofen | |
|---|---|---|---|---|
| | Value | Source | Value | Source |
| *Diffusion Layer Model parameters* | | | | |
| Particle handling model | PPB | PPB | PPB | |
| Particle $h_{eff}$ model | Fluid dynamics | Fluid dynamics | Fluid dynamics | |
| PSD | Polydispersed | Polydispersed | Polydispersed | |
| Particles density (g/mL) | 1.2 (default) | 1.2 (default) | 1.2 (default) | |
| Mean particle radius (μm) | 20 [41] | 20 [41] | 123 [19] | |
| Particle radius range (μm) | 0.5–50 [41] | 0.5–50 [41] | 31–311 [19] | |

MW: molecular weight; $S_0$: intrinsic solubility; B/P: blood-to-plasma ratio; $f_{u,plasma}$: fraction unbound in plasma; ADAM: advanced dissolution, absorption and metabolism; $P_{app}$: apparent permeability; $P_{eff,man}$: human jejunum effective permeability; ka: absorption rate constant; $f_{u,GUT}$: fraction unbound in enterocytes; ARS: absorption rate scalar; $V_{ss}$: volume of distribution at steady state; Kp: tissue-to-plasma partition coefficient; $CL_{int}$: intrinsic clearance; $V_{max}$: maximum enzymatic reaction rate; $K_M$: substrate concentration at half $V_{max}$; CYP: cytochrome P450; UGT: UDP-glucuronosyl transferase; HLM: human liver microsomes; $CL_R$: renal clearance; PPB: particle population balance; PSD: particle size distribution.

### 2.4. Model evaluation

Initial graphical assessment of simulated *vs* observed concentration–time profiles was performed to verify the predictive performance of the PBPK framework. Additionally, following metrics (Equations 1–4) assessing accuracy and precision of the outputs were computed to numerically assess the predictive power of the PBPK models developed:

- Prediction Error (PE):

$$PE = \frac{Pred_i}{Obs_i} \quad (1)$$

- Average Fold Error (AFE):

$$AFE = 10^{\frac{1}{n}\sum \log\frac{Pred_i}{Obs_i}} \quad (2)$$

- Absolute Average Fold Error (AAFE):

$$AAFE = 10^{\frac{1}{n}\sum \left|\log\frac{Pred_i}{Obs_i}\right|} \quad (3)$$

- Percent Prediction Error (PPE%):

$$PPE(\%) = Mean\left(\left|\frac{Pred_i - Obs_i}{Obs_i}\right| \times 100\right) \quad (4)$$

Where $Pred_i$ and $Obs_i$ are the predicted and observed PK parameter been evaluated, respectively. In general, model predictions were considered excellent if $0.9 \leq$ AFE/PE $\leq 1.1$, satisfactory if $0.8 \leq$ AFE/PE $\leq 1.25$, acceptable if $0.5 \leq$ AFE/PE $< 0.8$ or $1.25 <$ AFE/PE $\leq 2$ and poor if AFE/PE $< 0.5$ or AFE/PE $> 2$. Following the same rationale, AAFE $\leq 1.1$, AAFE $\leq 1.25$, $1.25 <$ AAFE $\leq 2$ and AAFE $> 2$ were considered excellent, satisfactory, acceptable and poor, respectively. For PPE%, the lower the value, the better the prediction.

### 2.5. Model application

The developed PBPK models for oral suspensions were used to assess the impact of different PSD in systemic exposure of each enantiomer after the administration of two formulations (test and reference) containing a racemic mixture of ibuprofen. Reference formulation PSD was kept as that corresponding to the developed DLM. Mean radius of suspended particles of the test formulations was increased by a factor of 10 and 45 to simulate different scenarios with lower dissolution rate. Three representative scenarios were generated varying the PSD: (i) test formulation with a 20 % lower $C_{max}$ compared to the $C_{max}$ of the reference formulation; (ii) test formulation with a $T_{max}$ equal to 50 min (~20 % decrease on $T_{maxREF}$); and (iii) test formulation with a $T_{max}$ equal to 70 min (~20 % increase on $T_{maxREF}$). Deterministic simulations using a population representative of the HV population of Simcyp® were performed. Ratios test/reference (T/R) were calculated using different PK parameters: area under the concentration–time profile from zero to last observation ($AUC_{0\text{-}t}$), area under the concentration–time profile from zero to median $T_{max}$ of the reference ($AUC_{Tmax}$), $C_{max}$ and $T_{max}$.

## 3. Results

Fig. 1 depicts the observed *vs* predicted $AUC_{0\text{-}t}$ and $C_{max}$ for each ibuprofen enantiomer of the 54 scenarios (27 for each enantiomer) from 11 Phase I clinical trials. Numerical assessment of the predictive performance (accuracy through AFE and precision through AAFE) for both exposure PK parameters (i.e., $AUC_{0\text{-}t}$ and $C_{max}$) of the PBPK models is shown in Table 3. For R-ibuprofen, 48 % (13/27) and 96 % (26/27) of PE in $AUC_{0\text{-}t}$ fell within the 0.9–1.1 and 0.8–1.25 range, respectively, whereas for $C_{max}$ 44 % (12/27) and 67 % (18/27) of PE fell in the 0.9–1.1 and 0.8–1.25 range, respectively. For S-ibuprofen, 67 % (18/27) and 96 % (26/27) of PE in $AUC_{0\text{-}t}$ fell within the 0.9–1.1 and 0.8–1.25 range, respectively, whereas for $C_{max}$ 67 % (18/27) and 100 % (27/27) of PE fell in the 0.9–1.1 and 0.8–1.25 range, respectively. Graphical assessment of longitudinal PK profiles of ibuprofen enantiomers during model development (supplementary material Figures 6–11) and model verification (Fig. 2) after the IV infusion and oral administration of liquid and solid formulations were performed.

### 3.1. IV formulation

As depicted in Fig. 2*A*, disposition processes of both enantiomers were well described by the PBPK model, with most of the observations (81 % for R-ibuprofen and 85 % for S-ibuprofen) falling between the 5th and 95th percentiles of the simulated profiles regardless of the dose level (400 and 600 mg) and the infusion time (15, 20 and 30 min). Both, the estimated racemase $CL_{int}$ (87.25 μL/min/mg protein) (see Table 3 of supplementary material) and the optimised HLM additional $CL_{int}$ (70 μL/min/mg protein) were confirmed in all 4 studies (A-D) and the optimisation of the Kp scalar to 1.5 with data from study A was also confirmed in study B. Predicted *versus* observed R- and S-ibuprofen concentration–time profiles after the IV administration of 100 mg of R-ibuprofen can be found in Figure 12 of supplementary material. Moreover, the verified PBPK model also confirmed the non-linear and stereoselective plasma protein binding of ibuprofen enantiomers. The PBPK model showed high accuracy and precision predicting the exposure PK parameters $AUC_{0\text{-}t}$ and $C_{max}$ of R- and S-ibuprofen after the IV infusion of 400 and/or 600 mg of racemic ibuprofen, with most of the PE (3/6 in $AUC_{0\text{-}t}$ and 5/6 in $C_{max}$) falling in the 0.9–1.10 range and all within the

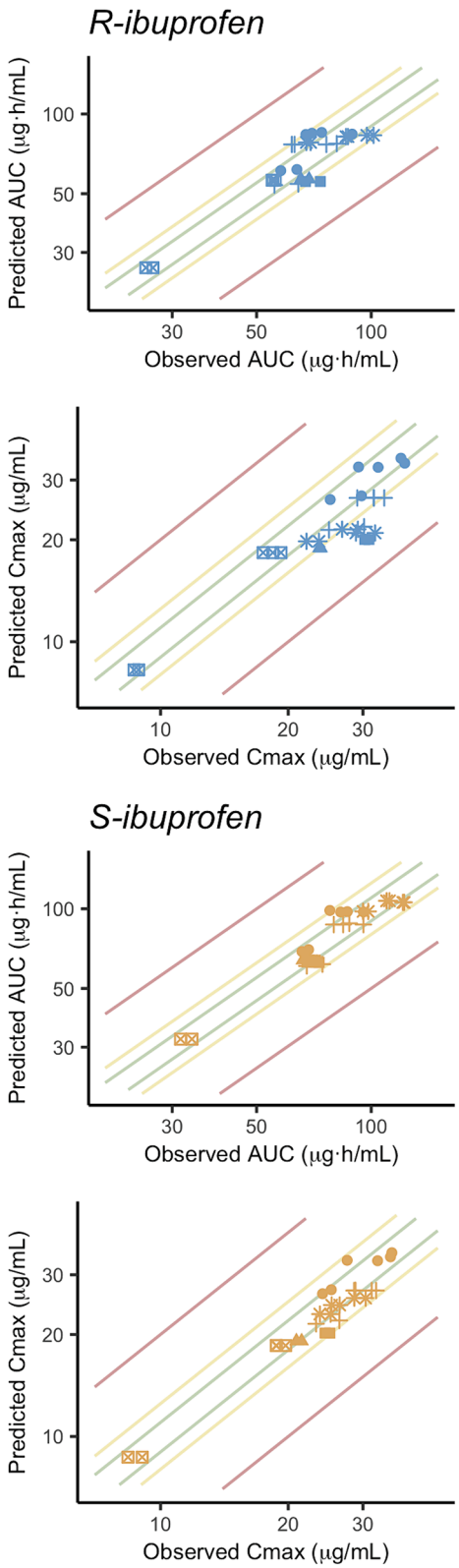


**Fig. 1.** Observed *versus* predicted exposure PK parameters $AUC_{0\text{-}t}$ and $C_{max}$ for R- (blue) and S-ibuprofen (golden). Circles: solution for infusion; plus symbols: oral solution; crossed squares: oral suspension; triangles: soft gelatine capsules; filled squares: soft gelatine capsule with lysine; asterisks: tablets. Green, yellow, and red lines represent the 0.9–1.10, 0.8–1.25 and 0.5–2 prediction error ranges, respectively. (For interpretation of the references to colour in this figure legend, the reader is referred to the web version of this article.)

0.8–1.25 range. The model also showed excellent accuracy (AFE) and precision (AAFE), with PPE well below 15 % for $AUC_{0\text{-}t}$ and of 7 % for $C_{max}$ (see Table 3). Additionally, the PBPK model was able to predict the lack of dose proportionality observed, with PE for the ratios of dose-normalized $AUC_{0\text{-}t}$ and $C_{max}$ of 400 mg over 600 mg of 0.90 and 0.99 for R-ibuprofen, respectively, and 0.91 and 1.04 for S-ibuprofen, respectively.

### 3.2. Oral solution

A similar trend was observed after the simulation of the oral administration of solutions containing racemic ibuprofen-arginine (Fig. 2*B*), with all the PE in $AUC_{0\text{-}t}$ for both enantiomers falling within the 0.8–1.25 range. Numerical predictive check showed 79 % and 83 % of R- and S-ibuprofen observations, respectively, falling between the 5th and 95th percentiles of the simulated profiles. Moreover, 3/6 $AUC_{0\text{-}t}$ PE and 1/6 $C_{max}$ PE for R-ibuprofen were within 0.9–1.1 range. In the case of the eutomer (i.e., S-ibuprofen) the PBPK model predicted 5/6 $AUC_{0\text{-}t}$ PE and 3/6 $C_{max}$ PE matching the 0.9–1.1 range. High accuracy (AFE) and precision (AAFE) to predict the systemic exposure of ibuprofen enantiomers was obtained, with PPE well below 15 % in all cases, apart from R-ibuprofen $C_{max}$ (PPE of 17 %). PK profiles of both enantiomers after the administration of 200 mg of R-ibuprofen as oral solution are shown in supplementary material Figure 13.

### 3.3. Oral suspension

Successful model performance (76 % of R- and 78 % of S-ibuprofen observations within the 5th and 95th percentiles of the simulated profiles) was observed when simulating the administration of oral suspensions with different ibuprofen concentrations (i.e., 2 and 4 %) (Fig. 2*C*), as almost all (19/20) of the PE computed for both enantiomers and PK exposure parameters fell within the 0.9–1.1 range (Table 3). The DLM within the ADAM model developed showed excellent accuracy (AFE) and precision (AAFE) in the prediction of R- and S-ibuprofen exposure, with PPE well below 10 % (Table 3).

### 3.4. Soft gelatine capsules

Fig. 2*D* shows the graphic evaluation of the predictive power of the developed PBPK model for ibuprofen enantiomers after the oral administration of soft gelatine capsules. Keeping the parameterisation of the DLM model developed for the oral suspension as well as the optimised ARS as a function of the ibuprofen salt, the simulations corresponding to the administration of a soft capsule with and without lysine in their composition covered most of the observed data within the 5th and 95th percentiles of the simulated profiles (72 % of observations for both enantiomers). Notwithstanding, a small bias was observed in the prediction of R-ibuprofen exposure after the administration of soft capsules of racemic ibuprofen containing lysine salt, as observed mean profiles were between the 50th and 95th of the simulated profiles. This was confirmed through the numerical assessment of the predictive power of the PBPK models for ibuprofen enantiomers (Table 3), as the PBPK model for S-ibuprofen showed better performance, with all the PE in $AUC_{0\text{-}t}$ and $C_{max}$ between 0.8–1.25 and PPE well below 20 %, while R-ibuprofen exposure prediction was slightly biased as revealed by the PPE in $AUC_{0\text{-}t}$ (21 %) and in $C_{max}$ (35 %). Lower accuracy and precision in the prediction of R-ibuprofen exposure was confirmed with AFE and AAFE of 0.79 and 1.26, respectively, for $AUC_{0\text{-}t}$ and 0.65 and 1.53, respectively, for $C_{max}$. For soft gelatine capsules without lysine in their composition, R-ibuprofen exposure was better predicted by the model, with AFE and AAFE of 0.85 and 1.18, respectively, for $AUC_{0\text{-}t}$ and 0.80 and 1.26, respectively, for $C_{max}$. Globally, the PBPK model better predicted the exposure to the eutomer (S-ibuprofen) than to the distomer (R-ibuprofen) for these rapid oral absorption IR solid formulations.

**Table 3**
Numerical assessment of the PBPK model for R-ibuprofen and S-ibuprofen.

| Ibuprofen enantiomer | PK endpoint | Formulation | N | Dose (mg) | N 0.9–1.10(%) | N 0.8–1.25(%) | AFE | AAFE | PPE (%) |
|---|---|---|---|---|---|---|---|---|---|
| R-ibuprofen | $AUC_{0-t}$ | Solution for infusion | 6 | 400, 600 | 3 (50 %) | 6 (100 %) | 1.09 | 1.12 | 13 |
| | | Oral Sol. ARG | 6 | 400, 600 | 3 (50 %) | 6 (100 %) | 1.03 | 1.12 | 12 |
| | | Oral Susp. | 5 | 200, 400 | 5 (100 %) | 5 (100 %) | 1.01 | 1.02 | 2 |
| | | Soft Caps. LYS | 2 | 400 | 0 (0 %) | 1 (50 %) | 0.79 | 1.26 | 21 |
| | | Soft Caps. | 2 | 400 | 0 (0 %) | 2 (100 %) | 0.85 | 1.18 | 15 |
| | | Tablet | 6 | 600 | 2 (33 %) | 6 (100 %) | 0.97 | 1.13 | 12 |
| | $C_{max}$ | Solution for infusion | 6 | 400, 600 | 5 (83 %) | 6 (100 %) | 0.98 | 1.07 | 7 |
| | | Oral Sol. ARG | 6 | 400, 600 | 1 (16.6 %) | 4 (66,6%) | 0.82 | 1.21 | 17 |
| | | Oral Susp. | 5 | 200, 400 | 5 (100 %) | 5 (100 %) | 0.98 | 1.05 | 4 |
| | | Soft Caps. LYS | 2 | 400 | 0 (0 %) | 0 (0 %) | 0.65 | 1.53 | 35 |
| | | Soft Caps. | 2 | 400 | 0 (0 %) | 2 (100 %) | 0.80 | 1.26 | 20 |
| | | Tablet | 6 | 600 | 1 (16 %) | 3 (50 %) | 0.77 | 1.30 | 22 |
| S-ibuprofen | $AUC_{0-t}$ | Solution for infusion | 6 | 400, 600 | 3 (50 %) | 5 (83 %) | 1.11 | 1.11 | 11 |
| | | Oral Sol. ARG | 6 | 400, 600 | 5 (83 %) | 6 (100 %) | 0.96 | 1.09 | 8 |
| | | Oral Susp. | 5 | 200, 400 | 4 (80 %) | 5 (100 %) | 0.94 | 1.07 | 7 |
| | | Soft Caps. LYS | 2 | 400 | 0 (0 %) | 2 (100 %) | 0.87 | 1.15 | 13 |
| | | Soft Caps. | 2 | 400 | 2 (100 %) | 2 (100 %) | 0.95 | 1.05 | 5 |
| | | Tablet | 6 | 600 | 4 (67 %) | 6 (100 %) | 0.95 | 1.06 | 6 |
| | $C_{max}$ | Solution for infusion. | 6 | 400, 600 | 5 (83 %) | 6 (100 %) | 1.06 | 1.07 | 7 |
| | | Oral Sol. ARG | 6 | 400, 600 | 3 (50 %) | 6 (100 %) | 0.89 | 1.13 | 11 |
| | | Oral Susp. | 5 | 200, 400 | 5(100 %) | 5 (100 %) | 0.98 | 1.03 | 3 |
| | | Soft Caps. LYS | 2 | 400 | 0 (0 %) | 2 (100 %) | 0.82 | 1.23 | 18 |
| | | Soft Caps. | 2 | 400 | 1(50 %) | 2 (100 %) | 0.90 | 1.11 | 10 |
| | | Tablet | 6 | 600 | 4 (67 %) | 6 (100 %) | 0.92 | 1.09 | 8 |

$AUC_{0-t}$: area under the concentration–time profile from zero to last observation; Oral Sol. ARG: oral solution of the arginine salt of racemic ibuprofen; Oral Susp.: oral suspension or racemic ibuprofen acid; Soft Caps. LYS: soft gelatine capsules of the lysine salt of racemic ibuprofen; Soft Caps.: soft gelatine capsules of racemic ibuprofen acid; N: number of scenarios; N 0.9–1.10: number of prediction errors between 0.9–1.10; N 0.8–1.25: number of prediction errors between 0.8–1.25; N 0.5–2: number of prediction errors between 0.5–2; AFE: average fold error; AAFE: absolute average fold error; PPE: percent prediction error.

### 3.5. Tablets

The administration of tablets containing 600 mg of racemic ibuprofen was also adequately described by the model, with 56 % of R- and 70 % of S-ibuprofen observations falling within the 5th and 95th percentiles of the simulated profiles (Fig. 2*E*). The simulated dose administered for S-ibuprofen was 350 mg, 16.67 % higher than the value corresponding to 50 % of the total dose. This increase in the dose of the eutomer was a direct consequence of the hepatic first pass effect on R-ibuprofen (chiral inversion). Notwithstanding, PE in $AUC_{0-t}$ and $C_{max}$ for R-ibuprofen were within the 0.8–1.25 range in 100 % (6/6) and 50 % (3/6), respectively, of the scenarios. For S-ibuprofen both, $AUC_{0-t}$ and $C_{max}$, were within the 0.9–1.1 range in 66 % (4/6) and within the 0.8–1.25 PE range in all cases. The PBPK frameworks developed showed excellent accuracy and precision in the prediction of S-ibuprofen exposure and R-ibuprofen $AUC_{0-t}$ as revealed by AFE and AAFE (Table 3), with PPE in S-ibuprofen $AUC_{0-t}$, $C_{max}$ and R-ibuprofen $AUC_{0-t}$ of 6 %, 8 % and 12 %, respectively. However, a small bias was observed in the prediction of R-ibuprofen $C_{max}$, with AFE, AAFE and PPE of 0.77, 1.30 and 22 %, respectively.

### 3.6. Model application

Based on the results from Table 4, R-ibuprofen is the most sensitive analyte to detect differences in PSD for oral suspensions containing a racemic mixture of ibuprofen. The T/R ratio (%) of $C_{max}$ for R- and S-ibuprofen were 77.27 and 80.00, respectively, suggesting the absorption rate of the distomer is more sensitive to changes in absorption rate due to changes in dissolution rate. However, for test formulations with 10 min change in $T_{max}$, both enantiomers provided similar ratios across the PK parameters $AUC_{0-t}$ and $C_{max}$.

When assessing the sensitivity of the conventional PK parameters ($AUC_{0-t}$, $C_{max}$ and $T_{max}$) to detect differences in PSD, $T_{max}$ has been identified as the most sensitive PK parameter. When a PSD generating a 20 % decrease in $C_{max}$ was assumed, 84.15 % change on $T_{max}$ for both enantiomers was observed. On the other hand, when $T_{max}$ was changed by 10 min (increasing or decreasing), 1–3 % variation on $C_{max}$ was predicted, respectively. This illustrates that $T_{max}$ is more discriminative than $C_{max}$. $AUC_{0-t}$ ratios (100 %) are not relevant for anticipating BE as ibuprofen is completely absorbed regardless of dissolution rate of immediate release products. When comparing $T_{max}$ with $AUC_{Tmax}$, $T_{max}$ is more discriminative when the absorption rate is increased to obtain $T_{max}$ 10 min earlier (point estimates of 84 % for $T_{max}$ and 110 % for $AUC_{Tmax}$), whereas $AUC_{Tmax}$ is more discriminative when the absorption rate is reduced to obtain $T_{max}$ 10 min later (point estimates of 117 % for $T_{max}$ and 76 % for $AUC_{Tmax}$). Both changes in $T_{max}$ and $AUC_{Tmax}$ are irrespective of the enantiomer of ibuprofen.

## 4. Discussion

A genuine and innovative PBPK model of ibuprofen enantiomers including mechanistic dissolution and absorption, as well as stereoselectivity in disposition processes, has been successfully developed and verified using a hierarchical workflow with different intravenous and oral formulations containing a racemic mixture of ibuprofen. The disposition processes of ibuprofen enantiomers were adequately characterized using a minimal PBPK structure, which has been successfully applied for the characterization of other NSAIDs and their use is supported for BE assessment from a regulatory perspective [45]. Besides the inclusion of CYP- and UGT-mediated metabolism of ibuprofen [18], the model not only implements different metabolic rates for each enantiomer (i.e., stereoselectivity), but also, and more importantly, it considers the unidirectional inversion of R-ibuprofen to S-ibuprofen. This latter process is determinant when accounting for the elimination of the distomer. The performance of our PBPK model to predict ibuprofen enantiomers PK outcomes in the 0.8–1.25 PE range is very high for oral suspensions (100 %) and oral solutions (92 %), high for tablets (88 %), and moderate for soft gelatine capsules (69 %). The PBPK model predicted complete absorption ($f_a = 1$) and high bioavailability (84 %), indicating the extent of absorption is not relevant for evaluating dissolution changes. Thus, the use of these highly predictive PBPK models for anticipating BE outcomes is sufficiently endorsed.

Stereoselectivity has been incorporated in terms of different fraction unbound in plasma and enzymatic kinetic parameters and metabolic

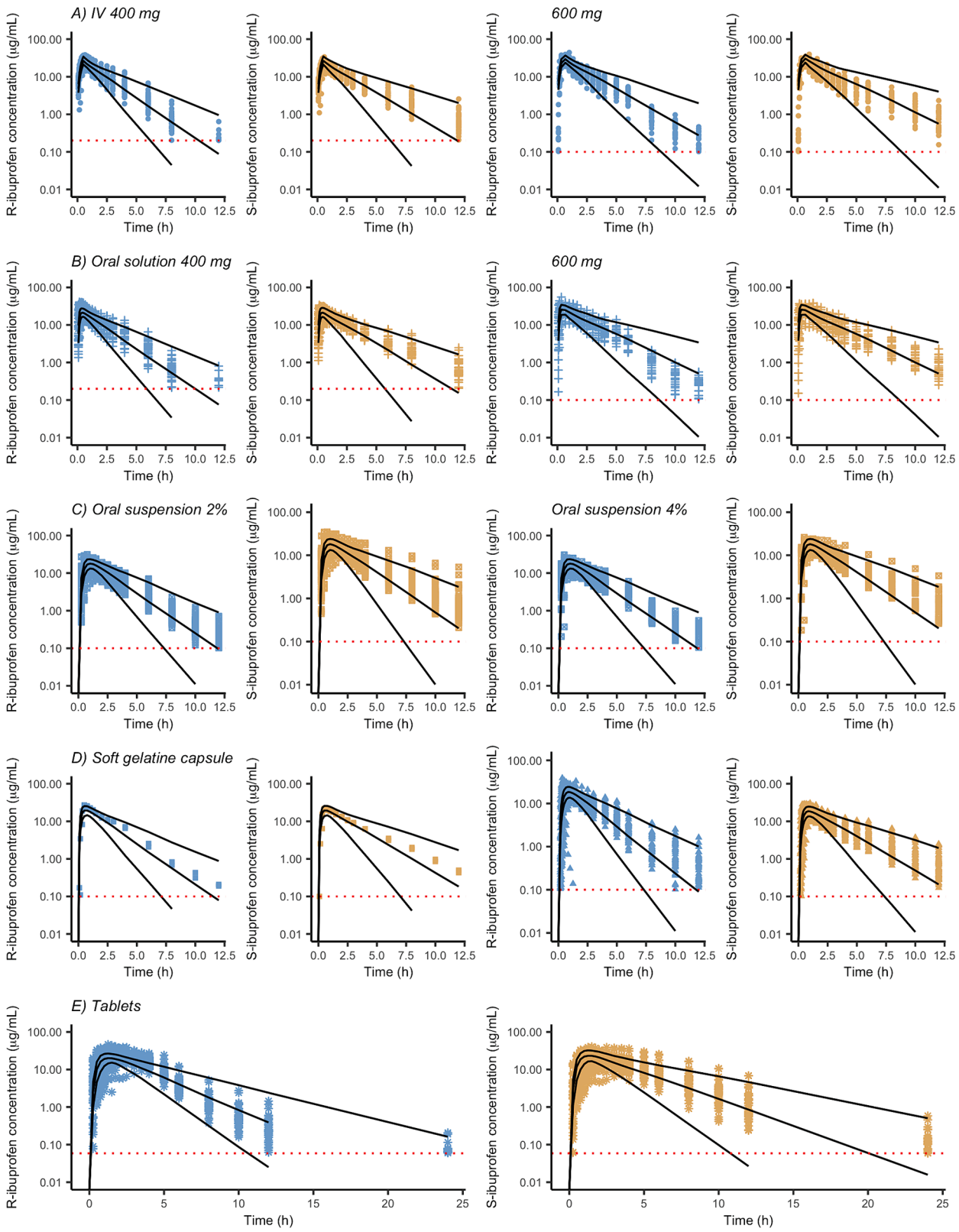


**Fig. 2.** Observed *versus* predicted plasma concentration–time profiles of R- (blue) and S-ibuprofen (golden) after the A) IV infusion and oral administration of B) solutions with arginine, C) 2 % and 4 % suspensions (400 mg), D) soft gelatine capsules with (left) and without (right) lysine (400 mg) and E) tablets (600 mg) of racemic ibuprofen. Black profiles indicate the 5th, 50th and 95th percentiles of the simulated profiles in the model verification step. Horizontal dotted red lines indicate lower limit of quantification of the analytical method used to quantify ibuprofen enantiomers. (For interpretation of the references to colour in this figure legend, the reader is referred to the web version of this article.)

**Table 4**
Deterministic assessment of bioequivalence outcomes as a consequence of changes in particle size distribution.

| | | | $C_{max}$ (µg/mL | $T_{max}$ (h) | $AUC_{0-t}$ (µg·h/mL) | $AUC_{Tmax}$ (µg·h/mL) |
|---|---|---|---|---|---|---|
| **Test $C_{max}$ 80 %** | S-ibu | Ref | 16.40 | 1.01 | 52.87 | 10.03 |
| | | Test | 13.12 | 1.86 | 55.05 | 3.63 |
| | | T/R (%) | 80.00 | 184.15 | 104.12 | 36.19 |
| | R-ibu | Ref | 16.28 | 1.01 | 48.73 | 9.92 |
| | | Test | 12.58 | 1.86 | 48.88 | 3.63 |
| | | T/R (%) | 77.27 | 184.15 | 100.30 | 36.59 |
| **Test $T_{max}$ 50 min** | S-ibu | Ref | 16.40 | 1.01 | 52.87 | 10.03 |
| | | Test | 16.63 | 0.85 | 52.71 | 11.10 |
| | | T/R (%) | 101.40 | 84.16 | 99.70 | 110.67 |
| | R-ibu | Ref | 16.28 | 1.01 | 48.73 | 9.92 |
| | | Test | 16.51 | 0.85 | 48.74 | 11.00 |
| | | T/R (%) | 101.41 | 84.16 | 100.00 | 110.89 |
| **Test $T_{max}$ 70 min** | S-ibu | Ref | 16.40 | 1.01 | 52.87 | 10.03 |
| | | Test | 15.94 | 1.18 | 53.28 | 7.67 |
| | | T/R (%) | 97.19 | 116.83 | 100.78 | 76.47 |
| | R-ibu | Ref | 16.28 | 1.01 | 48.73 | 9.92 |
| | | Test | 15.75 | 1.18 | 48.85 | 7.66 |
| | | T/R (%) | 96.74 | 116.83 | 100.25 | 77.22 |

S-Ibu: S-ibuprofen; R-Ibu: R-ibuprofen; T/R: test over reference formulation ratio as percentage; Test $C_{max}$ 80 %: test formulation with a 20 % lower $C_{max}$ compared to the $C_{max}$ of the reference formulation; Test $T_{max}$ 50 min: test formulation with a $T_{max}$ equal to 50 min (~20 % decrease on $T_{maxREF}$); Test $T_{max}$ 70 min: test formulation with a $T_{max}$ equal to 70 min (~20 % increase on $T_{maxREF}$); $AUC_{0-t}$: area under the concentration–time profile from zero to last observation; $AUC_{Tmax}$: area under the concentration–time profile from zero to median $T_{max}$ of the reference formulation.

pathways for CYP2C8 and CYP2C9 for each enantiomer. Chiral inversion of 2-arylpropionic NSAIDs represents a relevant pathway for the elimination of the inactive R-enantiomer [46]. Accordingly, the unidirectional chiral inversion of R-ibuprofen to S-ibuprofen has been characterized estimating an intrinsic clearance through a cytosolic racemase that would simplify the complexity of this process (stereoselective enzymatic activation of R-ibuprofen to R-ibuprofenyl-adenylate followed by an acyl coenzyme A thioester formation and final epimerization yielding both, R- and S-ibuprofen) [38]. To account for the variability in R-to-S unidirectional inversion through the cytosolic racemase in HVs, 81.033 mg/g ± 21.467 % were considered as the mean value of cytosolic protein per gram of liver and the default %CV available in Simcyp®, respectively. Then, the liver weight considered for each virtual HV was used to ultimately calculate the R-to-S unidirectional inversion in the whole liver. The predicted mass balance derived from our simulations showed 52 % of the dose administered as R-ibuprofen is inverted to S-ibuprofen and elimination through this racemase accounts for 55 % of the systemic clearance of this enantiomer (see Figure 14 and Table 5 of supplementary material). These results are strongly supported by the literature, as population PK analyses have estimated R-ibuprofen clearance by inversion reaction in 60 % [39] and it has been reported an average of 53–65 % of R-ibuprofen inversion in humans [38]. The higher metabolic rate of R-ibuprofen is consistent with already published reports [47], resulting in a 13 % longer half-life for S-ibuprofen (1.83 h *vs* 2.11 h). Additionally, the lack of dose proportionality has also been modelled through a non-linear $f_u$ in plasma and with a higher Kp scalar for 600 mg), resulting in a 26 % higher $V_{ss}$ for this dose level when compared to 400 mg. The plasma protein binding saturation and the lack of dose proportionality can be found elsewhere [38]. The high accuracy (AFE) in the prediction of both $AUC_{0-t}$ and $C_{max}$ for R-ibuprofen (1.09 and 0.98, respectively) and for S-ibuprofen (1.11 and 1.06, respectively), as well as the precision (AAFE) of this model structure in the prediction of $AUC_{0-t}$ (1.12 for R-ibuprofen and 1.11 for S-ibuprofen) and $C_{max}$ (1.07 for both enantiomers) after the IV infusion of a racemic mixture of ibuprofen strongly supports the modeling of the disposition processes mentioned above and the stereoselectivity incorporated in plasma protein binding and metabolic reactions.

The ADAM model [34] has been used to mechanistically characterize the absorption process. $P_{eff,man}$ was predicted from Caco-2 $P_{app}$ ($52.5 \cdot 10^{-6}$ cm/s) and assumed to be the same for both enantiomers. The segregated transit time model has been selected to split the transit times along the gastrointestinal tract as a function of particle size for all the oral formulations considered. In this regard, fluid and dissolved drug, as well as fine particles mean residence time in the stomach were reduced from an initial value of 0.27 h to 0.12 h to better describe the observed $T_{max}$ among the formulations assessed. This was a direct consequence of the extremely short $T_{max}$ observed for the oral solution (0.25–0.5 h). The impact of amino acids (lysine and arginine) in the solubility and absorption of ibuprofen has been previously reported [38] and prompted the increase of the ARS in duodenum and jejunum to 10 to better characterize the enhanced absorption of ibuprofen in the proximal segments of the gastrointestinal tract, where the ADAM model showed maximum absorption. Assuming no chiral inversion of R-ibuprofen in the gut and the unbound fraction in the enterocyte predicted by Simcyp®, the PBPK model accurately predicted R- (83 %) and S-ibuprofen (84 %) bioavailability [38,47]. The ADAM model parameterization together with the previous verified disposition processes allowed an accurate (all AFE in the range 0.8–1.25) and precise (all AAFE below 1.25) description of the exposure of both enantiomers after the administration of the racemic ibuprofen-arginate in solution.

The DLM was used to mechanistically characterize the dissolution process of different IR oral formulations. The pH-dependent solubility was modelled with the intrinsic solubility and a solubility factor of 79 to describe the two phases and the plateau observed in the solubility profile *in vitro* [14]. Similar to $P_{eff,man}$ and $CL_R$, no differentiation was incorporated in terms of solubility for ibuprofen enantiomers, as this parameter is unlikely affected when dissolving in a non-chiral solvent/environment. The solubility at the particle surface accounted for the self-buffering effect of ibuprofen dissolution, changing the pH in the particle surface, thus generating a gradient of pH as a function of the radius and conditioning dissolution rate. With this assumption, particle surface pH and bulk pH were modelled independently, which has been identified as crucial for properly describing ibuprofen dissolution and absorption [48]. The PPB model was used to simulate a PSD with different mean radius for oral suspension (20 µm) and tablets (123 µm) (see Table 2). Oral suspension formulations were best described with the PBPK model in terms of accuracy and precision (see AFE and AAFE values in Table 3), with PPE as high as 7 %. This strongly verifies model performance and supports the use of this framework for performing BE outcome assessments with confidence. The last rapid oral absorption formulation (i.e., soft gelatine capsules with and without lysine) was properly described by the PBPK model for S-ibuprofen, with AFE and AAFE values for $AUC_{0-t}$ and $C_{max}$ between 0.8–1.25 and lower than 1.25, respectively (see Table 3 for more details). In the case of R-ibuprofen, exposure PK parameters were slightly biased, with PPE higher than 20 % in all cases (see Table 3). However, a common factor was found in the prediction of PK outcomes: formulations containing lysine in their composition tend to be biased, especially when predicting $C_{max}$. This is in line with our previous findings about the effect of arginine in absorption rate and it is likely due to the lack of mechanistic insight in the absorption process (further than a simple ARS). Tablets are the most complex formulations among IR oral formulations as they must disintegrate and disaggregate to release the drug and make it available to dissolve and, consequently, to get absorbed. This, obviously, increases $T_{max}$ and slows absorption rate. In this line, it has been reported that ibuprofen absorption rate influences R-to-S unidirectional inversion [30,49,50], suggesting longer residence time in the gastrointestinal tract would lead to higher S/R

concentration ratios. Despite there is also evidence about the R-to-S inversion in excised segments of human ileum and colon [31], we could not clarify this process based on our data since the ADAM model predicted almost complete absorption (93 %) before reaching the ileum. Notwithstanding, our PBPK model is able to predict the S/R ratio after the IV and oral administration of R-ibuprofen (Figures 15 and 16 of supplementary material). Taking all the above mentioned and our model structure, we hypothesize R-to-S chiral inversion is a saturable process that mainly takes place in the liver, as the cancellation of the racemase activity in the intestine did not impact simulation outcomes and S-ibuprofen formation from R-ibuprofen was accurately predicted in the model development step (see supplementary material Figure 13). Racemase kinetic behavior has been modelled through a $CL_{int}$ instead of a $V_{max}$ and $K_M$ to avoid identifiability issues. This is not a concern when simulating the oral administration of IR formulations with high absorption rates such as solutions, suspensions, or soft capsules, as the racemase would be saturated and the percentage of inversion of R-ibuprofen because of hepatic first pass effect would be negligible, and no virtual dose adjustment for S-ibuprofen when simulating the administration of a racemic mixture is needed. For complex formulations with slower absorption rates (i.e., tablets), racemase would work far from saturation, inverting more R-ibuprofen to S-ibuprofen as it firstly passes through the liver. Consequently, it was necessary to increase the dose of S-ibuprofen administered by 16.67 % (50 mg) to mimic the amount of R-ibuprofen inverted as a consequence of its hepatic first pass effect (pre-systemic inversion) because of the low absorption rate of this formulation. This hypothesis was confirmed with the accuracy and precision of the PBPK model in predicting S-ibuprofen exposure, with AFE and AAFE of 0.95 and 1.06, respectively, for $AUC_{0\text{-}t}$ and 0.92 and 1.09, respectively, for $C_{max}$.

Based on the satisfactory predictive performance of the current PBPK model for oral suspensions of ibuprofen (100 % of the studies for $C_{max}$ and 90 % of the studies for AUC within the 0.9–1.1 range), a BE risk assessment using the typical predicted PK profile was conducted to evaluate the impact of PSD on the PK outcomes of both enantiomers. R-ibuprofen has emerged as the most sensitive analyte to detect differences in PSD for suspensions containing 400 mg of ibuprofen (Table 4). Currently, ibuprofen product-specific bioequivalence guidelines from the FDA and EMA allow bioequivalence to be demonstrated using achiral bioanalytical methods. When $T_{max}$ is considered as a primary PK parameter (e.g., in the EU), the use of a chiral bioanalytical method is not necessary, since the mixture of enantiomers is as sensitive as the eutomer (S-Ibuprofen $T_{max}$ T/R and R-Ibuprofen $T_{max}$ T/R ratios of 84.16 % for $T_{max}$ 10 min earlier or 116.83 % for $T_{max}$ 10 min later). However, when $T_{max}$ is not considered as a primary PK parameter (e.g., in the USA) the achiral method is over-discriminative compared to the eutomer (S-Ibuprofen $C_{max}$ T/R ratio of 80.00 % *vs* R-Ibuprofen $C_{max}$ T/R ratio of 77.27 %), since the outcome of the mixture of enantiomers will be located in between the outcome of both enantiomers. Therefore, products that show equivalence for the eutomer may fail to show equivalence with the mixture of both enantiomers as determined with the achiral method. In summary, the use of an achiral bioanalytical method does not represent an increased risk of bioinequivalence for the patients, but an inflation of the risk of concluding non-equivalence when the products are actually equivalent for the eutomer. However, this small inflation of the type II error (i.e., the probability of getting false negative results) is compensated by the use of a simpler and cheaper bioanalytical method.

Where onset of action is considered clinically relevant (e.g., in the EU), $T_{max}$ is generally the most sensitive PK parameter amongst those used in the EU for BE assessment (i.e. $AUC_{0\text{-}t}$, $C_{max}$ and $T_{max}$) to detect differences in rate of absorption caused by differences in PSD of ibuprofen suspensions. However, $AUC_{Tmax}$ is more discriminative than $T_{max}$ when the test product exhibits a slower rate of absorption.

Although some discrepancies exist regarding the presence of pre-systemic chiral inversion of R-ibuprofen in humans [30,31,49,50], the lack of experimental information after the administration of R-ibuprofen in formulations with different absorption rates did not allow to fully mechanistically describe (with $V_{max}$ and $K_M$ values) this process in the proposed PBPK models. So, setting the intestinal racemase activity scalar to 0 must be handled with caution as more data are needed to mechanistically describe and place this process. Due to structural limitations of Simcyp®, it was not possible to simulate the administration of the racemic mixture (i.e., each enantiomer handled as a substrate) or adding the formed S-ibuprofen from R-ibuprofen to the dose administered as S-ibuprofen. Consequently, no displacement interaction on plasma protein binding between enantiomers could be considered. The large dataset used in this work comes from 11 independent clinical trials performed in different countries, facilities and by different sponsors and personnel, which increased the variability of the observed PK data. Despite the large experimental evidence collected across the different Phase I studies, the lack of multiple-dose regimen studies represents a limitation of the PBPK model to predict steady-state concentrations of each enantiomer in different oral formulations and evaluate their potential impact on bioequivalence.

In conclusion, the developed and verified framework represents a milestone in the field of PBPK M&S, since it is the first PBPK model addressing stereospecific properties of ibuprofen in ADME processes and based on experimental information obtained in a wide range of IR oral formulations. Moreover, the proposed PBPK model satisfactorily accounts for the interplay between complex PK processes (non-linear plasma protein binding) and the unidirectional R-to-S inversion, anticipating the relevance of R-ibuprofen as the most sensitive analyte for bioequivalence evaluation of oral suspensions of ibuprofen, which supports the use of achiral bioanalytical methods for demonstration of bioequivalence of ibuprofen suspensions, and identifying $T_{max}$ as the most discriminative PK parameter when comparing the rate of absorption of ibuprofen suspensions. The bioequivalence risk assessment guided by the proposed PBPK model would represent a useful strategy to evaluate the impact of critical dissolution- and absorption-related parameters of oral formulations containing racemic ibuprofen for regulatory purposes, consolidating a predictive in silico framework that can reduce and refine future bioequivalence studies.

## CRediT authorship contribution statement

**Javier Reig-López:** Writing – review & editing, Writing – original draft, Methodology, Formal analysis, Data curation. **Marina Cuquerella-Gilabert:** Writing – review & editing, Writing – original draft, Methodology, Formal analysis, Data curation, Conceptualization. **Enrique Bandín-Vilar:** Writing – review & editing. **Matilde Merino-Sanjuán:** Writing – review & editing, Supervision, Formal analysis. **Víctor Mangas-Sanjuán:** Writing – review & editing, Writing – original draft, Supervision, Formal analysis, Conceptualization. **Alfredo García-Arieta:** Writing – review & editing, Writing – original draft, Supervision, Formal analysis, Conceptualization.

## Declaration of Competing Interest

The authors declare that they have no known competing financial interests or personal relationships that could have appeared to influence the work reported in this paper.

## Data availability

The authors do not have permission to share data.

## Appendix A. Supplementary material

Supplementary data to this article can be found online at https://doi.org/10.1016/j.ejpb.2024.114293.

## References


[1] S. Krishnaswami, D. Austin, M.R. Gastonguay, J. Gobburu, P.H. van der Graaf, D. Ouellet, S. Tannenbaum, S.A.G. Visser, MID3: mission impossible or model-informed drug discovery and development? point-counterpoint discussions on key challenges, Clin. Pharmacol. Ther. 107 (2020) 762–772, https://doi.org/10.1002/cpt.1788.

[2] EFPIA MID3 Workgroup, S.F. Marshall, R. Burghaus, V. Cosson, S.Y.A. Cheung, M. Chenel, O. DellaPasqua, N. Frey, B. Hamren, L. Harnisch, F. Ivanow, T. Kerbusch, J. Lippert, P.A. Milligan, S. Rohou, A. Staab, J.L. Steimer, C. Tornoe, S.A.G. Visser, Good Practices in Model-Informed Drug Discovery and Development: Practice, Application, and Documentation, CPT Pharmacometrics Syst. Pharmacol. 5 (2016) 93-122. 10.1002/psp4.12049.

[3] S. Marshall, R. Madabushi, E. Manolis, K. Krudys, A. Staab, K. Dykstra, S.A. G. Visser, Model-informed drug discovery and development: current industry good practice and regulatory expectations and future perspectives, CPT Pharmacometrics Syst. Pharmacol. 8 (2019) 87–96, https://doi.org/10.1002/psp4.12372.

[4] E. Manolis, J. Brogren, S. Cole, J.L. Hay, A. Nordmark, K.E. Karlsson, F. Lentz, N. Benda, G. Wangorsch, G. Pons, W. Zhao, V. Gigante, F. Serone, J.F. Standing, A. Dokoumetzidis, J. Vakkilainen, M. van den Heuvel, V. Mangas Sanjuan, J. Taminiau, E. Kerwash, D. Khan, F.T. Musuamba, I. Skottheim Rusten, EMA modelling and simulation working group, commentary on the MID3 good practices paper, CPT Pharmacometrics Syst. Pharmacol. 6 (2017) 416–417, https://doi.org/10.1002/psp4.12223.

[5] M. Jamei, Recent advances in development and application of physiologically-based pharmacokinetic (PBPK) models: a transition from academic curiosity to regulatory acceptance, Curr. Pharmacol. Rep. 2 (2016) 161–169, https://doi.org/10.1007/s40495-016-0059-9.

[6] W. Lin, Y. Chen, J.D. Unadkat, X. Zhang, D. Wu, T. Heimbach, Applications, challenges, and outlook for PBPK Modeling and simulation: a regulatory, industrial and academic perspective, Pharmaceutical Research 1 (2022), https://doi.org/10.1007/s11095-022-03274-2.

[7] P. Zhao, L. Zhang, J.A. Grillo, Q. Liu, J.M. Bullock, Y.J. Moon, P. Song, S.S. Brar, R. Madabushi, T.C. Wu, B.P. Booth, N.A. Rahman, K.S. Reynolds, E. Gil Berglund, L. J. Lesko, S.M. Huang, Applications of physiologically based pharmacokinetic (PBPK) modeling and simulation during regulatory review, Clin. Pharmacol. Ther. 89 (2011) 259–267, https://doi.org/10.1038/clpt.2010.298 [doi].

[8] L. Kuepfer, C. Niederalt, T. Wendl, J. Schlender, S. Willmann, J. Lippert, M. Block, T. Eissing, D. Teutonico, Applied concepts in PBPK modeling: how to build a PBPK/PD model, CPT Pharmacometrics Syst. Pharmacol. 5 (2016) 516–531, https://doi.org/10.1002/psp4.12134.

[9] A.N. Edginton, F. Theil, W. Schmitt, S. Willmann, Whole body physiologically-based pharmacokinetic models: their use in clinical drug development, Expert Opin. Drug Metab. Toxicol. 4 (2008) 1143–1152, https://doi.org/10.1517/17425255.4.9.1143.

[10] H.M. Jones, I.B. Gardner, K.J. Watson, Modelling and PBPK simulation in drug discovery, Aaps J. 11 (2009) 155–166, https://doi.org/10.1208/s12248-009-9088-1.

[11] US Food and Drug Administration, Physiologically Based Pharmacokinetic Analyses - Format and Content Guidance for Industry (2018) https://www.fda.gov/regulatory-information/search-fda-guidance-documents/physiologically-based-pharmacokinetic-analyses-format-and-content-guidance-industry.

[12] US Food and Drug Administration, The Use of Physiologically Based Pharmacokinetic Analyses–Biopharmaceutics Applications for Oral Drug Product Development, Manufacturing Changes, and Controls (2020) https://www.fda.gov/regulatory-information/search-fda-guidance-documents/use-physiologically-based-pharmacokinetic-analyses-biopharmaceutics-applications-oral-drug-product.

[13] European Medicines Agency, Reporting of physiologically based pharmacokinetic (PBPK) modelling and simulation - Scientific guideline (2018) https://www.ema.europa.eu/en/reporting-physiologically-based-pharmacokinetic-pbpk-modelling-simulation-scientific-guideline.

[14] H. Potthast, J.B. Dressman, H.E. Junginger, K.K. Midha, H. Oeser, V.P. Shah, H. Vogelpoel, D.M. Barends, Biowaiver monographs for immediate release solid oral dosage forms: ibuprofen, J. Pharm. Sci. 94 (2005) 2121–2131, https://doi.org/10.1002/jps.20444.

[15] A. García-Arieta, J. Gordon, H. Potthast, On the biopharmaceutics classification system biowaiver of ibuprofen, J. Pharm. Sci. 104 (2015) 2429–2432, https://doi.org/10.1002/jps.24519.

[16] R. Cristofoletti, J.B. Dressman, Dissolution methods to increasing discriminatory power of in vitro dissolution testing for ibuprofen free acid and its salts, J. Pharm. Sci. 106 (2017) 92–99, https://doi.org/10.1016/j.xphs.2016.06.001.

[17] R. Cristofoletti, J.B. Dressman, Bridging the gap between in vitro dissolution and the time course of ibuprofen-mediating pain relief, J. Pharm. Sci. 105 (2016) 3658–3667, https://doi.org/10.1016/j.xphs.2016.08.024.

[18] R. Cristofoletti, J.B. Dressman, Use of physiologically based pharmacokinetic models coupled with pharmacodynamic models to assess the clinical relevance of current bioequivalence criteria for generic drug products containing Ibuprofen, J. Pharm. Sci. 103 (2014) 3263–3275, https://doi.org/10.1002/jps.24076.

[19] R. Cristofoletti, B. Hens, N. Patel, V.V. Esteban, S. Schmidt, J. Dressman, Integrating drug- and formulation-related properties with gastrointestinal tract variability using a product-specific particle size approach: case example ibuprofen, J. Pharm. Sci. 108 (2019) 3842–3847, https://doi.org/10.1016/j.xphs.2019.09.012.

[20] R. Cristofoletti, J.B. Dressman, Matching phosphate and maleate buffer systems for dissolution of weak acids: equivalence in terms of buffer capacity of bulk solution or surface pH? Eur. J. Pharm. Biopharm. 103 (2016) 104–108, https://doi.org/10.1016/j.ejpb.2016.03.024.

[21] R. Cristofoletti, J.B. Dressman, FaSSIF-V3, but not compendial media, appropriately detects differences in the peak and extent of exposure between reference and test formulations of ibuprofen, Eur. J. Pharm. Biopharm. 105 (2016) 134–140, https://doi.org/10.1016/j.ejpb.2016.06.004.

[22] I. Camara-Martinez, J.A. Blechar, A. Ruiz-Picazo, A. Garcia-Arieta, C. Calandria, V. Merino-Sanjuan, P. Langguth, M. Gonzalez-Alvarez, M. Bermejo, J. Al-Gousous, I. Gonzalez-Alvarez, Level A IVIVC for immediate release tablets confirms in vivo predictive dissolution testing for ibuprofen, Int. J. Pharm. 614 (2022) 121415, https://doi.org/10.1016/j.ijpharm.2021.121415.

[23] S.S. Adams, P. Bresloff, C.G. Mason, Pharmacological differences between the optical isomers of ibuprofen: evidence for metabolic inversion of the (-)-isomer, J. Pharm. Pharmacol. 28 (1976) 256–257, https://doi.org/10.1111/j.2042-7158.1976.tb04144.x.

[24] G. Geisslinger, K.P. Stock, G.L. Bach, D. Loew, K. Brune, Pharmacological differences between R(-)- and S(+)-ibuprofen, Agents Actions 27 (1989) 455–457, https://doi.org/10.1007/BF01972851.

[25] A.M. Evans, Enantioselective pharmacodynamics and pharmacokinetics of chiral non-steroidal anti-inflammatory drugs, Eur. J. Clin. Pharmacol. 42 (1992) 237–256, https://doi.org/10.1007/BF00266343.

[26] M. Villanueva, R. Heckenberger, H. Strobach, M. Palmer, K. Schror, Equipotent inhibition by R(-)-, S(+)- and racemic ibuprofen of human polymorphonuclear cell function in vitro, Br. J. Clin. Pharmacol. 35 (1993) 235–242, https://doi.org/10.1111/j.1365-2125.1993.tb05690.x.

[27] J. Caldwell, A.J. Hutt, S. Fournel-Gigleux, The metabolic chiral inversion and dispositional enantioselectivity of the 2-arylpropionic acids and their biological consequences, Biochem. Pharmacol. 37 (1988) 105–114, https://doi.org/10.1016/0006-2952(88)90762-9.

[28] M. Simonyi, On chiral drug action, Med. Res. Rev. 4 (1984) 359–413, https://doi.org/10.1002/med.2610040304.

[29] A.J. Hutt, J. Caldwell, The metabolic chiral inversion of 2-arylpropionic acids–a novel route with pharmacological consequences, J. Pharm. Pharmacol. 35 (1983) 693–704, https://doi.org/10.1111/j.2042-7158.1983.tb02874.x.

[30] F. Jamali, N.N. Singh, F.M. Pasutto, A.S. Russell, R.T. Coutts, Pharmacokinetics of ibuprofen enantiomers in humans following oral administration of tablets with different absorption rates, Pharm. Res. 5 (1988) 40–43, https://doi.org/10.1023/a:1015811428066.

[31] F. Jamali, R. Mehvar, A.S. Russell, S. Sattari, W.W. Yakimets, J. Koo, Human pharmacokinetics of ibuprofen enantiomers following different doses and formulations: intestinal chiral inversion, J. Pharm. Sci. 81 (1992) 221–225, https://doi.org/10.1002/jps.2600810306.

[32] M. Jamei, S. Marciniak, D. Edwards, K. Wragg, K. Feng, A. Barnett, A. Rostami-Hodjegan, The simcyp population based simulator: architecture, implementation, and quality assurance, In. Silico Pharmacol. 1 (2013) 9, https://doi.org/10.1186/2193-9616-1-9.

[33] M. Jamei, S. Marciniak, K. Feng, A. Barnett, G. Tucker, A. Rostami-Hodjegan, The Simcyp population-based ADME simulator, Expert Opin. Drug Metab. Toxicol. 5 (2009) 211–223, https://doi.org/10.1517/17425250802691074.

[34] M. Jamei, D. Turner, J. Yang, S. Neuhoff, S. Polak, A. Rostami-Hodjegan, G. Tucker, Population-based mechanistic prediction of oral drug absorption, Aaps J. 11 (2009) 225–237, https://doi.org/10.1208/s12248-009-9099-y.

[35] J.K. Paliwal, D.E. Smith, S.R. Cox, R.R. Berardi, V.A. Dunn-Kucharski, G.H. Elta, Stereoselective, competitive, and nonlinear plasma protein binding of ibuprofen enantiomers as determined in vivo in healthy subjects, J. Pharmacokinet. Biopharm. 21 (1993) 145–161, https://doi.org/10.1007/BF01059767.

[36] T. Rodgers, M. Rowland, Physiologically based pharmacokinetic modelling 2: predicting the tissue distribution of acids, very weak bases, neutrals and zwitterions, J. Pharm. Sci. 95 (2006) 1238–1257, https://doi.org/10.1002/jps.20502.

[37] T. Rodgers, D. Leahy, M. Rowland, Physiologically based pharmacokinetic modeling 1: predicting the tissue distribution of moderate-to-strong bases, J. Pharm. Sci. 94 (2005) 1259–1276.

[38] N.M. Davies, Clinical pharmacokinetics of ibuprofen. the first 30 years, Clin. Pharmacokinet. 34 (1998) 101–154, https://doi.org/10.2165/00003088-199834020-00002.

[39] J. Lotsch, U. Muth-Selbach, I. Tegeder, K. Brune, G. Geisslinger, Simultaneous fitting of R- and S-ibuprofen plasma concentrations after oral administration of the racemate, Br. J. Clin. Pharmacol. 52 (2001) 387–398, https://doi.org/10.1046/j.1365-2125.2001.01451.x.

[40] H. Cheng, J.D. Rogers, J.L. Demetriades, S.D. Holland, J.R. Seibold, E. Depuy, Pharmacokinetics and bioinversion of ibuprofen enantiomers in humans, Pharm. Res. 11 (1994) 824–830, https://doi.org/10.1023/a:1018969506143.

[41] J.C. Rivera-Leyva, M. Garcia-Flores, A. Valladares-Mendez, L.M. Orozco-Castellanos, M. Martinez-Alfaro, Comparative studies on the dissolution profiles of oral ibuprofen suspension and commercial tablets using biopharmaceutical classification system criteria, Indian, J. Pharm. Sci. 74 (2012) 312–318, https://doi.org/10.4103/0250-474X.107062.

[42] S. Yee, In vitro permeability across Caco-2 cells (colonic) can predict in vivo (small intestinal) absorption in man–fact or myth, Pharm. Res. 14 (1997) 763–766, https://doi.org/10.1023/a:1012102522787.

[43] S. Chang, W. Li, S.C. Traeger, B. Wang, D. Cui, H. Zhang, B. Wen, A.D. Rodrigues, Confirmation that cytochrome P450 2C8 (CYP2C8) plays a minor role in (S)-(+)-

and (R)-(-)-ibuprofen hydroxylation in vitro, Drug Metab. Dispos. 36 (2008) 2513–2522, https://doi.org/10.1124/dmd.108.022970.
[44] G.E. Kuehl, J.W. Lampe, J.D. Potter, J. Bigler, Glucuronidation of nonsteroidal anti-inflammatory drugs: identifying the enzymes responsible in human liver microsomes, Drug Metab. Dispos. 33 (2005) 1027–1035, https://doi.org/10.1124/dmd.104.002527.
[45] I. Loisios-Konstantinidis, R. Cristofoletti, N. Fotaki, D.B. Turner, J. Dressman, Establishing virtual bioequivalence and clinically relevant specifications using in vitro biorelevant dissolution testing and physiologically-based population pharmacokinetic modeling. case example: Naproxen, Eur. J. Pharm. Sci. 143 (2020) 105170, https://doi.org/10.1016/j.ejps.2019.105170.
[46] H. Ikuta, A. Kawase, M. Iwaki, Stereoselective pharmacokinetics and chiral inversion of ibuprofen in adjuvant-induced arthritic rats, Drug Metab. Dispos. 45 (2017) 316–324, https://doi.org/10.1124/dmd.116.073239.
[47] E. Gonzalez-Rojano, J. Marcotegui, L. Laredo, L. Gwaza, J. Gordon, A. Portoles, E. Vargas, S. Morales-Alcelay, A. Garcia-Arieta, Chiral bioanalytical methods in bioequivalence studies of intravenous vs. oral formulations of ibuprofen, Chirality 32 (2020) 1169–1177, https://doi.org/10.1002/chir.23258.
[48] B. Hens, N. Seegobin, M. Bermejo, Y. Tsume, N. Clear, M. McAllister, G.E. Amidon, G.L. Amidon, Dissolution challenges associated with the surface ph of drug particles: integration into mechanistic oral absorption modeling, Aaps J. 24 (2022) 17, https://doi.org/10.1208/s12248-021-00663-0.
[49] G. Ding, Y. Liu, J. Sun, Y. Takeuchi, T. Toda, T. Hayakawa, S. Fukushima, S. Kishimoto, W. Lin, N. Inotsume, Effect of absorption rate on pharmacokinetics of ibuprofen in relation to chiral inversion in humans, J. Pharm. Pharmacol. 59 (2007) 1509–1513, https://doi.org/10.1211/jpp.59.11.0007.
[50] D. Siemon, J.X. de Vries, F. Stotzer, I. Walter-Sack, R. Dietl, Fasting and postprandial disposition of R(-)- and S(+)-ibuprofen following oral administration of racemic drug in healthy individuals, Eur. J. Med. Res. 2 (1997) 215–219.